Advances in Research

17(6): 1-16, 2018; Article no.AIR.43283
ISSN: 2348-0394, NLM ID: 101666096

Effect of Dust Deposition on the Quantum Efficiency of BPS150-36 Polycrystalline Silicon Photovoltaic Modules during Winter Months in Pahou, Benin

Minadohona Maxime Capo-Chichi[1,2], Basile Bruno Kounouhéwa[1,2], Vianou Irénée Madogni[1,2*] and Macaire Agbomahéna[3]

[1]Département de Physique (FAST) et Formation Doctorale Sciences des Matériaux (FDSM), Université d'Abomey-Calavi, Bénin.
[2]Laboratoire de Physique du Rayonnement LPR, FAST-UAC, 01 BP 526 Cotonou, Bénin.
[3]Laboratoire de Caractérisation Thermophysique des Matériaux et Appropriation Energétique (Labo CTMAE/EPAC/UAC), Abomey-Calavi, Bénin.

Authors' contributions

This work was carried out in collaboration between all authors. Authors MMCC and BBK developed the general idea of the present research, also carrying out the literature review and manuscript preparation at early stages. The methodology and analytic procedures were carried out by author VIM. Final review, including final manuscript correction has been done by author BBK. All authors were in charge of data generation/analysis and post-processing of the results. All authors read and approved the final manuscript.

Article Information

DOI: 10.9734/AIR/2018/43283
Editor(s):
(1) Dr. Prashant Kumar, Assistant Professor, Department of Electrical Engineering, Zeal College of Engineering and Research, Savitribai Phule Pune University, India.
(2) Dr. Francisco Marquez-Linares, Professor of Chemistry, Nanomaterials Research Group, School of Science and Technology, University of Turabo, USA.
Reviewers:
(1) Hermes José Loschi, State University of Campinas (UNICAMP), Campinas, Brazil.
(2) Chandra Bhal Singh, School of Materials Science and Technology, Indian Institute of Technology (BHU), India.
(3) Abdelkader Djelloul, Centre de Recherche en Technologie des Semi-conducteurs pour l'Energétique (CRTSE), Algeria.
(4) Hafiz Muhammad Ali, University of Engineering and Technology, Taxila, Pakistan.
(5) Wanninayake, WMNMB, Horizon University, Sri Lanka.
Complete Peer review History: http://www.sciencedomain.org/review-history/27956

Original Research Article

Received 12 July 2018
Accepted 29 September 2018
Published 24 December 2018

ABSTRACT

Dust is the lesser acknowledged factor that significantly influences the performance of the PV cells/modules.
We investigated analytically from optical models, the performance degradation of the BPS150-36

**Corresponding author: E-mail: madognimadogni@gmail.com;*

Polycrystalline silicon module, caused by the natural dust deposition effects on the transparent panel surface.
We modeled, a system (Air-dust-glass) formed of a dust layer supposed opaque and formed of several thousand small grains of different sizes settled on the glass surface. The Matrix-Transfer theory with the cubic spline interpolation method has been exploited for data correlation. Matlab software has been used to results in numerical simulation.
The results obtained show a decrease in PV output intensity, the supply voltage and therefore the power output. That strongly depends on dust thickness on the panel's surface over a period of three months.
The drop in PV cell quantum efficiency is directly caused by the dust accumulation, trees debris and bird's droppings on the cells/modules surface. The meteorological conditions, the installations quality and the geographical position of PV cells/modules can also influence the photovoltaic process. These factors have not been taken into account in our model.

Keywords: Degradation; dust depositing effect; matrix-transfer theory; drop; meteorological conditions; photovoltaic process.

1. INTRODUCTION

PV cells/modules are currently highly used in rural electrification, and grid connected systems, in a water pumping irrigation, and remote checkpoint mostly in the arid areas where the peoples have not accessed to conventional electricity. Owing to their versatility, low maintenance, and long lifetime, PV modules are an alternative solution for small, off the grid energy projects especially in underdeveloped countries, mainly Benin. Recently, the use of these devices in the tropical and desert regions has increased strongly [1]. These devices are degraded by several extrinsic factors (humidity, temperature, dust, atmospheric pressure, wind and snow, breakage and cracks in the cells, delamination and bubbles, and longtime ultraviolet (UV) illumination), which reduces the intrinsic lifetime of the devices very short [2,3].

Tropical middles, mainly Benin are the hottest and dusty areas where the dust represents the main barrier to PV utilization. So, tiny particles of sand, trees debris, and bird's droppings are accumulating on the surface of PV modules [4], which yield shading sunlight on modules, the consequence a significant power loss as shown in Fig. 1.

It is very important to study the extrinsic factors (humidity, dust, temperature, solar irradiance, wind speed, etc) that affect the PV cells/modules performance owing to their increasing use in the hot, dusty and humid climate region [5].

Dust is a general term for any particulate matter less than 500 mm in diameter, which is about the dimension of an optical fiber used for communications or 10 times the diameter of a human hair. Dust can comprise small amounts of pollen (vegetation, fungi, bacteria), human/animal cells, hair, carpet and textile fibers (sometimes termed microfibers), and, most commonly, organic minerals from geomorphic fallout such as sand, clay, or eroded limestone [6-8]. Atmospheric dust (aerosols) is attributed to various sources, such as soil elements lifted by the wind (Aeolian dust), volcanic eruptions, vehicle movement, and pollution. The particle size, constituents, and shape of the dust vary from region to region throughout the world. Furthermore, the deposition behaviour and accumulation rates can change dramatically in different localities [9].

Fig. 1. Trees debris and bird's droppings are accumulated on the surface of PV modules (Visual Inspection)

Several studies investigated the effect of dust on PV modules performance [9-22]. Recently, [23] compare experimentally, the energy performance of two identical pairs of PV-panels: the first being

clean and the second being artificially polluted with ash, i.e. a byproduct of incomplete hydrocarbons' combustion mainly originating from thermal power stations and vehicular exhausts. They have shown that the impact of different mass deposition of ash on PV's energy performance which is decrease between the clean and polluted panels varying between 2.3% and 27% during a time period of 1h. A similar study by the same authors [24], systematic experimental study of the pollution deposition has been conducted to investigate the performance of two identical pairs of PV panels. The first panel is clean and the second being artificially polluted with three different types of air pollutants namely, red soil, limestone and carbonaceous fly-ash particles.

The experimental study has been carried out under the same environmental conditions (ambient temperature, solar radiation, humidity, etc). The authors found that the red soil deposition on the PV cell surfaces causes the most considerable impact on the PV cells performance and thus the highest generated energy reduction, followed first by the limestone and secondly by the carbon-based ash. Specifically, an amount of 0.35 g/m^2 of red soil deposition on the PV cells surfaces may reduce the generated energy by almost 7.5% while approximately the same deposition density for limestone 0.33 g/m^2 causes almost 4% energy reduction. On the other hand, even if almost doubling the pollutant mass for ash 0.63 g/m^2 the generated energy is decreased by only 2.3%. This may be explained owing to the colour, composition and used diameter range of red soil causing the PV-panel to operate with lower performance [24]. Kaldellis JK and Kapsali M [8] developed an analytical model to obtain reliable results concerning the expected effect of regional air pollution on the PV cells/modules performance. Air pollution represented by red soil, limestone and carbon-based ash related to previous study. They used experimental data concerning the dust effect on the PV modules energy yield in a more polluted from the air pollution urban environment to validate their proposed theoretical model.

Sand and dust particles deposition on the PV cells surface in dry region are presented with numerical and analytical models by Beattie et al. [25] and supported by a laboratory investigation of sand particles accumulation on a glass surface. Sand particles accumulation on the glass surface disposed horizontally is found to exponentially reduce the available area for transmission of incident photon [25]. In addition, dust is then a key factor but lesser acknowledged that significantly influences the performance of the PV modules.

In this work, the transfer matrix theory with the cubic spline interpolation method has been exploited to investigate the performance degradation of BPS150-36 Polycrystalline silicon module, caused by the dust depositing effects on the panel transparent surface. We modeled, a system (Air-dust-glass) formed of a dust layer supposed opaque, and formed of several thousand small grains, of different sizes settled on the glass surface.

Moreover, dust accumulation on the transparent surface of a photovoltaic solar cell has a damaging effect on the cell's transmittance, and the reduction in transmittance depends on the quantity of the settled dust. However, atmospheric aerosols play an important role in regulating the amount of solar radiation absorbed by the Earth's atmospheric system [20]. They reflect part of the incident solar radiation back to space and absorb part of the solar radiation, affecting the distribution of solar heating through the atmosphere. Dust deposited properties and their impacts on the PV modules performance are very difficult to investigate, and they depend strongly on much localized environmental.

The rest of this manuscript is organized as follows: the different types of dust used are described in Section 2. Subsequently, the factors influencing dust settlement, Band diagram and working principle of BPS150-36 Polycrystalline module, the stacking layers modeling, the Matrix-Transfer theory, the Model approximation, dust and light absorbance have been established and presented. Next, the results are analysed and discussed in section 3. Finally, in section 4, the conclusions and our perspectives are enumerated.

2. MATERIALS AND METHODS

2.1 Description of different types of dust (Visual inspection)

Five types of dust (red soil, carbonaceous fly-ash, sand, calcium carbonate and silica Gel) are widely used experimentally to investigate the effects of air pollution on PV-panels performance [7-12, 26] (Fig. 2).

Fig. 2. Different types of dust used in the literature: (a)-Carbonaceous fly-ash, (b)-Sand, (C)-red soil, (d)-silica Gel, (e)-calcium carbonate

First, Carbonaceous fly-ash mainly is originated from the incomplete combustion of hydrocarbons emitted from vehicular exhausts. Second, a common urban air pollutant, sand, which is a naturally occurring granular material composed of mineral particles and finely divided rock. The composition of sand is extremely variable, depending on the local rock sources and conditions and it is mainly used for civil construction activities [26]. Third, red soil which is obtained from dry land is investigated is used. Fourth silica Gel represents the most common constituent of sand in inland continental settings and non-tropical coastal settings [27]. Finally, calcium carbonate, which is a common form of sand, mostly been created over the past half billion years, by various forms of life like shellfish and coral [7,28].

In addition, dust particles have distinct transmittance indices; some are completely opaque, while others have a specific degree of transparency [1].

2.2 Factors Influencing Dust Settlement

The characteristics of dust depositing on PV systems depend on two important factors that influences each other: The dust property and the local environment. Moreover, some factors can also influence the dust deposition significantly on the panels surface (Fig. 3).

Dust deposition is extremely complex and challenging to practically comprehend given all the factors that influences dust settlement [6].

2.3 Band Diagram: Working Principle of PV Module

The module considered is an inorganic photovoltaic device represented by its band diagram (Fig. 4). His photon flux conversion into electrical energy is based on three mechanisms [29]:

- The incident photons absorption by the active material constituting the device;
- Electron-hole pairs creation in the semiconductor material;
- Collect of the charge-carriers photo-generated in the device.

An incident photon is absorbed in the photoactive semiconductor if the photon energy is higher than the bandgap (E_g) of the semiconductor. This excites an electron from the valence band to the conduction band leaving a positively charged hole in the valence band. The electron and hole are then extracted at the contacts to the outer circuit.

The power conversion efficiency ($\boldsymbol{\eta}$) is defined as:

$$\eta = \frac{J_{SC} \times V_{OC} \times FF}{P_{Light}} \times 100\% \quad (1)$$

Where, $\boldsymbol{J_{SC}}$: the short circuit current, V_{OC}: The open circuit voltage, FF: The fill Factor and P_{Light}: the power of the light source.

A small $\mathbf{E_g}$ is desirable to absorb as many photons as possible. However for photons with $\mathbf{hv} > \boldsymbol{E_g}$ the extra energy is lost per thermodynamic relaxation [29,30,31]. In general,

assuming solar light generation, the lower the bandgap, the higher the J_{SC} and the lower the V_{OC}, hence there is some optimal bandgap that maximizes the product of the J_{SC} and the V_{OC}. Using the principle of detailed balance, the maximum achievable efficiency for a single junction solar cell at room temperature to be 44% and the optimal bandgap to be 1.1eV [31]. Taking further losses into account, they furthermore showed that the highest attainable η for a single junction cell is 31% under practical circumstances.

2.4 Optical Modeling

2.4.1 Stacking layers modeling

We modeled a system of three layers (Air-dust-glass) stacked one over the other, formed of a dust layer supposed opaque (Fig. 5(a)). Our objective is to determine the transmission coefficient T_j and reflection coefficient R_j at each interface j in the structure under an incidence angle θ_j (Fig. 5(b)).

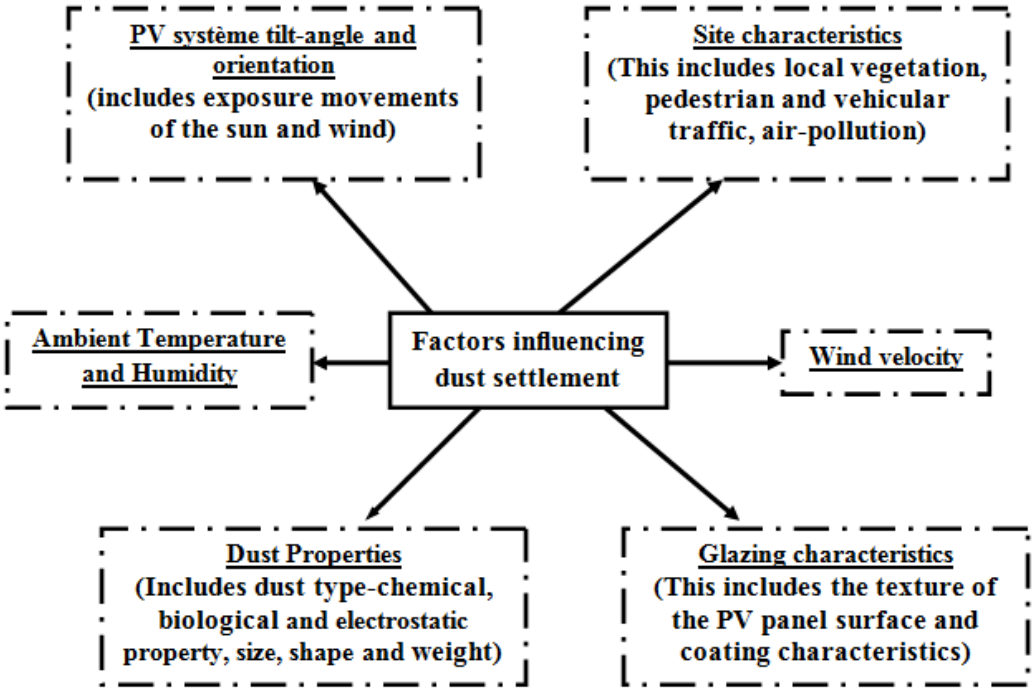

Fig. 3. Factors influencing dust settlement [6]

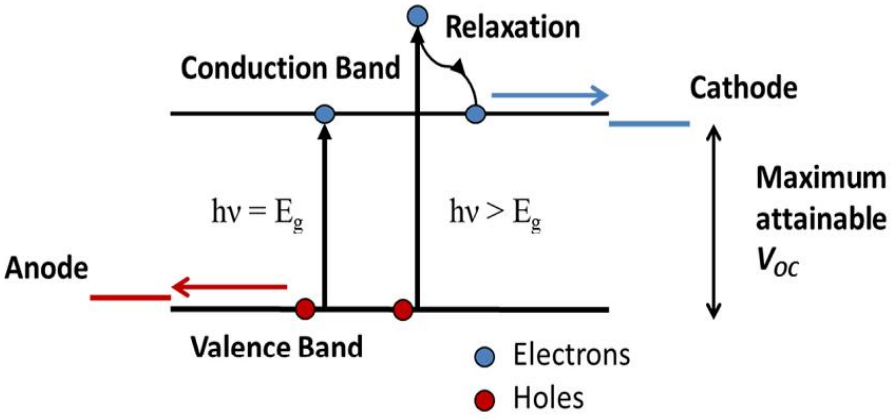

Fig. 4. Band diagram schematic of the solar cell considered [29,30]

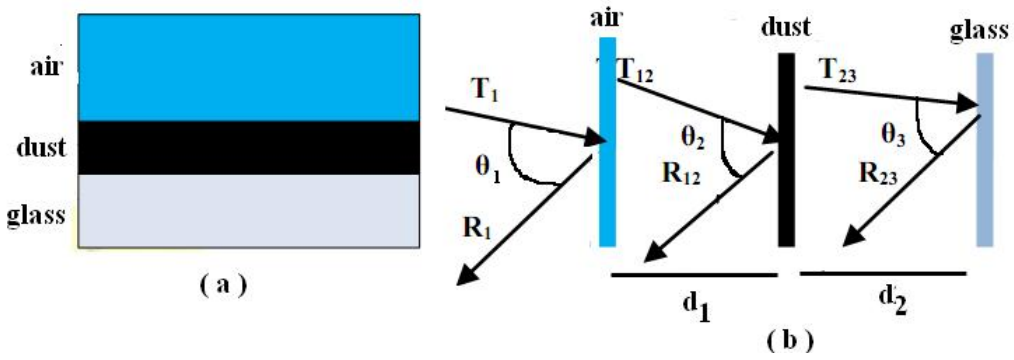

Fig. 5. Optical modeling of transmission and reflection phenomenon
(a)- Stacking layers structure, (b)- Optical modeling of the multilayer structure

2.4.2 Matrix-transfer theory

In this theory, we considered solely light under normal incidence. This case is representative under the standard conditions of the photovoltaic cells. We treated light as a plane wave which spreads, which transmitted and reflected at the interface j (Fig. 6). We assume that each layer j (j =1, 2,…, m) has a thickness d_j and optical properties described by a complex index of refraction. The optical electric field at any point in the system can be resolved into two components: one propagating in the positive x-direction and one in the negative x-direction, which, at a position x in layer j, are denoted $E_j^+(x)$ and $E_j^-(x)$, respectively [32, 33]. The total electric field in an arbitrary plane in layer j at a distance x to the right of boundary (j-1) j is given by:

$$E_j(x) = E_j^+(x) + E_j^-(x) \quad (2)$$

An interface matrix (refraction matrix) describes each interface in the structure.

$$I_{jk} = \frac{1}{t_{jk}} \begin{bmatrix} 1 & r_{jk} \\ r_{jk} & 1 \end{bmatrix} \quad (3)$$

Where r_{jk} and t_{jk} are the Fresnel complex reflection and transmission coefficients at interface jk.

For light with the electric field perpendicular to the plane of incidence (s-polarized or TE waves) the Fresnel complex reflection and transmission coefficients are defined by:

$$r_{jk} = \frac{q_j - q_k}{q_j + q_k} \quad \text{and} \quad t_{jk} = \frac{2q_j}{q_j + q_k} \quad (4)$$

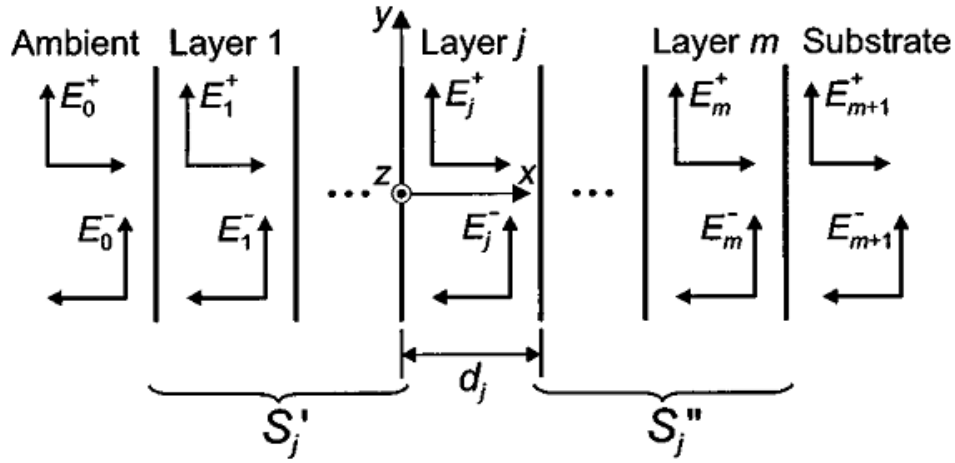

Fig. 6. A multilayer structure having m layers between a semi-infinite transparent substrate, an ambient substrate, and a semi-infinite substrate [32,33]

And for light with the electric field parallel to the plane of incidence (p-polarized or TM waves) as:

$$r_{jk} = \frac{\bar{n}_k^2 q_j - \bar{n}_j^2 q_k}{\bar{n}_k^2 q_j + \bar{n}_j^2 q_k} \text{ and } t_{jk} = \frac{2\bar{n}_j \bar{n}_k q_j}{\bar{n}_k^2 q_j + \bar{n}_j^2 q_k} \quad (5)$$

Where $q_j = \bar{n}_j cos\theta_j = [\bar{n}_j^2 - \bar{\eta}_o^2 sin\theta_o]^{\frac{1}{2}}$, and η_o : Refractive index of the transparent ambient, θ_o: Angle of incidence, and θ_j: Angle of refraction in layer j.

The layer matrix (phase matrix) describing the propagation through layer j is described by:

$$L_j = \begin{bmatrix} e^{-i\beta_j d_j} & 0 \\ 0 & e^{i\beta_j d_j} \end{bmatrix} \quad (6)$$

Where $\beta_j = \frac{2\pi}{\lambda} q_j$, and $\beta_j d_j$: The layer phase thickness corresponding to the phase change the wave experiences as it traverses layer j.

By considering the interface matrix and the layer matrix of Eq. (3) and Eq. (6), the total system transfer matrix S, which relates the electric field at ambient side and substrate side, is described by:

$$\begin{bmatrix} E_O^+ \\ E_O^- \end{bmatrix} = \boldsymbol{S} \begin{bmatrix} E_{m+1}^+ \\ E_{m+1}^- \end{bmatrix} \quad (7)$$

Can be written as:

$$\boldsymbol{S} = \begin{bmatrix} S_{11} & S_{12} \\ S_{21} & S_{22} \end{bmatrix} = \left(\coprod_{\nu=1}^{m} I_{(\nu-1)_\nu} L_\nu \right). I_{m\,(m+1)} \quad (8)$$

When light is incident from the ambient side in the positive x direction there is no wave propagating in the negative x direction inside the substrate, which means that $E_{m+1}^- = 0$. For the total layered structure the resulting complex reflection and transmission coefficients can be expressed by using the matrix elements of the total system transfer matrix of Eq. (8) as

$$r = \frac{E_O^-}{E_O^+} = \frac{S_{21}}{S_{11}} \quad \text{and} \quad t = \frac{E_{m+1}^+}{E_O^+} = \frac{1}{S_{11}} \quad (9)$$

In order to calculate the internal electric field in layer j the layer system can be divided into two subsets, separated by layer j, which means that the total system transfer matrix can be written as

$$S = S_j^{'} L_j S_j^{''} \quad (10)$$

The partial system transfer matrices for layer j are defined

$$\begin{bmatrix} E_O^+ \\ E_O^- \end{bmatrix} = \boldsymbol{S_j^{'}} \begin{bmatrix} E_j^{'+} \\ E_j^{'-} \end{bmatrix} \quad (11)$$

With $\boldsymbol{S_j^{'}}$ = $\begin{bmatrix} S_{j\,11}^{'} & S_{j\,12}^{'} \\ S_{j\,21}^{'} & S_{j\,22}^{'} \end{bmatrix} = \left(\coprod_{\nu=1}^{j-1} I_{(\nu-1)_\nu} L_\nu \right). I_{j\,(j-1)}$

Where $E_j^{'+}$ and $E_j^{'-}$ refer to the left boundary (j-1) j of layer j and

$$\begin{bmatrix} E_j^{''+} \\ E_j^{''-} \end{bmatrix} = \boldsymbol{S_j^{''}} \begin{bmatrix} E_{m+1}^+ \\ E_{m+1}^- \end{bmatrix} \quad (12)$$

With $\boldsymbol{S_j^{''}}$ = $\begin{bmatrix} S_{j\,11}^{''} & S_{j\,12}^{''} \\ S_{j\,21}^{''} & S_{j\,22}^{''} \end{bmatrix} = \left(\coprod_{\nu=j+1}^{m} I_{(\nu-1)_\nu} L_\nu \right). I_{m\,(m+1)}$

Where $E_j^{'+}$ and $E_j^{'-}$ refer to the right boundary j (j+1) of layer j. Also for the partial systems $\boldsymbol{S_j^{'}}$ and $\boldsymbol{S_j^{''}}$, it is possible to define complex reflection and transmission coefficients for layer j in terms of the matrix elements

$$\boldsymbol{r_j^{'}} = \frac{S_{j\,21}^{'}}{S_{j\,11}^{'}} \quad \text{and} \quad \boldsymbol{t_j^{'}} = \frac{1}{S_{j\,11}^{'}} \quad (13)$$

$$\boldsymbol{r_j^{''}} = \frac{S_{j\,21}^{'}}{S_{j\,11}^{'}} \quad \text{and} \quad \boldsymbol{t_j^{''}} = \frac{1}{S_{j\,11}^{''}} \quad (14)$$

Combining Eqs. (9) - (14), an internal transfer coefficient which relates the incident plane wave to the internal electric field propagating in the positive x direction in layer j at interface j (j - 1) can be derived as:

$$t_j^+ = \frac{E_j^+}{E_O^+} = \frac{t_j^{'}}{1 - r_{j-}^{'} . r_j^{''} . \exp(2i\beta_j d_j)} \quad (15)$$

where $r_{j-}^{'} = -\frac{S_{j\,12}^{'}}{S_{j\,11}^{'}}$.

An internal transfer coefficient which relates the incident plane wave to the internal electric field propagating in the negative x direction in layer j at interface (j-1) j can also be derived as:

$$t_j^- = \frac{E_j^-}{E_O^+} = \frac{t_j^{'} r_j^{''} . \exp(2i\beta_j d_j)}{1 - r_{j-}^{'} . r_j^{''} . \exp(2i\beta_j d_j)} = t_j^+ r_j^{''} . \exp(2i\beta_j d_j) \quad (16)$$

Using Eqs. (15) - (16), the total electric field in an arbitrary plane in layer j at a distance x to the right of boundary (j - 1) j in terms of the incident plane wave E_O^+ is giving by:

$$E_j(x) = \left[t_j^+ \exp\left(i\beta_j x\right) + t_j^- \exp\left(-i\beta_j x\right)\right]E_O^+ = t_j^+[\exp\left(i\beta_j x\right) + r_j^{''} \exp\left(i\beta_j\left(2d_j - x\right)\right)]E_O^+ \quad (17)$$

For $0 \le x \le d_j$ we have:

$$E_j(x) = \frac{s_{j\,11}^{''} \exp\left(-i\beta_j\left(d_j - x\right)\right) + s_{j\,21}^{''} \exp\left(i\beta_j\left(d_j - x\right)\right)}{s_{j\,11}^{'} s_{j\,11}^{''} \exp\left(-i\beta_j d_j\right) + s_{j\,12}^{'} s_{j\,21}^{''} \exp\left(i\beta_j d_j\right)} E_O^+ \quad (18)$$

2.4.3 Model approximation

We considered a harmonic propagation to describe the electromagnetic wave progression. Thus, the propagation equation of the electric field intensity coming from a light wave is given by:

$$\nabla\left(\frac{E_Z}{\mu_r}\right) - \left(\varepsilon_r - i\frac{\sigma}{\omega\,\varepsilon_0}\right)(k_0)^2 E_Z = 0 \quad (19)$$

Where, $\varepsilon_r = n^2$ σ : conductivity; ω : wave frequency; k_0 : wave vector; μ_r : Relative permeability; ε_0: Vacuum permittivity.

Optical interference effects to the different interfaces and inside of each layer are neglected in our model. Therefore, the generation rate or total solar intensity received by a clean photovoltaic cell is described as Casanova et al. [34], De et al. [35], Duffie and Beckman [36]:

$$G(\lambda, \theta) = I_0 \cos\theta + I_D \quad (20)$$

With I_0 : Direct radiation, I_D : Diffuse radiation and θ : inclination angle.

Next, we assumed that the efficiency losses in the modules induced by the dust are based on the hypothesis « dust grains ». Each dust grain is modeled in this model, as the divided homogeneously spheres on the panel surface. Each sphere has a reflection (**R**) and transmission (**T**) coefficient. At each interface, the reflection (R_j) and transmission (T_j) coefficient amplitudes are expressed:

- For light with the electric field perpendicular to the plane of incidence (s-polarized or TE waves);

$$R_{j-s} = \frac{n_{j-1}*cos\theta_j - 1 - n_j*cos\theta_j}{n_{j-1}*cos\theta_j - 1 + n_j*cos\theta_j} \quad (21)$$

$$T_{j-s} = \frac{2*n_{j-1}*cos\theta_j - 1}{n_{j-1}*cos\theta_j - 1 + n_j*cos\theta_j} \quad (22)$$

- For light with the electric field parallel to the plane of incidence (p-polarized or TM waves)

$$R_{j-p} = \frac{n_{j-1}*cos\theta_j - n_j*cos\theta_j}{n_{j-1}*cos\theta_j + n_j*cos\theta_j} \quad (23)$$

$$T_{j-p} = \frac{2*n_{j-1}*cos\theta_j - 1}{n_{j-1}*cos\theta_j + n_j*cos\theta_{j-1}} \quad (24)$$

Where J: Interface number in the structure.

Total amplitude of the reflection (R_j) and transmission (T_j) coefficient as a function of the dust grains radius (**r**) is expressed by:

$$R_j = \frac{r_j + r_{j+1}*\exp\left(-2i\beta_j\right)}{1 + r_j * r_{j+1}*\exp\left(-2i\beta_j\right)} \quad (25)$$

$$T_j = \frac{t_{j-1} * t_j * \exp\left(-2i\beta_{j-1}\right)}{1 + r_{j-1} * r_j * \exp\left(-2i\beta_j\right)} \quad (26)$$

With β_j: dephasing between the transmission and reflection of electromagnetic wave.

2.4.4 Dust and light absorbance

The main cause of the solar cells output power reduction is the attenuation in transmittance of light due to the dust accumulation on the glass cover [21]. The dust accumulation process is very easy it starts first by a simple layer accumulation until it covers all the surface, then a second layer will deposit on top of it and so on. To calculate the scattered light efficiency, we supposed that the dust particles are spherical and are composed mainly by SiO_2, thus the refractive index for the Silicon oxide as a function of the wavelength has been used. When these particles are illuminated they will absorb and scatter the light, which will reduce the intensity of the light beam, this effect is known as the extinction efficiency that is governed by the ratio of the particle size to the wavelength of the incident light [21,37]. The particle extinction efficiency can be obtained by combining the effects of scattering and absorption. The Mie theory can serve as the basis of the scattering and absorption of light as a function of the wavelength [37-40]. The calculation results of the light attenuation have been investigated by Sloane et al. [38], Bohren and Huffman [39], Van

[40] for different particle sizes ranging from 1 up to 5 μm diameter. They observed that particles with lower size (1 μm) scatter more light in the visible range of the solar spectrum than particle with high size.

This effect has been reported in Saito et al. [41], in which they would show that larger particles lead to more output due to the dependence of small particles to the light wavelength. We did not take into account in this work, the internal scattering between particles due to the computational limitation.

3. RESULTS AND DISCUSSION

3.1 Cells/modules Characteristics

PV module considered is constituted of 36 polycrystalline silicon cells (156 mm×156 mm), connected in series with a maximum power 150 Watts.

- Maximum supply voltage: 18V; Maximum power current: 8.33A;
- Open circuit-voltage: 21.60 V; Current short-circuit current: 9.08A
- Battery performance: 16.5%; Cells number (Pcs): 36;
- Size of portable : 156*156 mm; Module size: 1480*680*35 mm;
- Maximum system voltage : 1000 V; Fill factor (FF) $\geq 72\%$;
- Frame (material, corners, etc.) aluminum ; Output tolerance : $\pm 5\%$;
- Cable length : 900 mm; junction box type : PKJB001 (TUV);
- Weight per piece : 13 kg; Connectors and cables type: with TUV certificate;
- Maximum surface load capacity: 60 m/s (200 kg/m^2).

❖ ***Relative coefficients to the temperature:***

- Temperature coefficient of J_{SC} (%) : + 0,1/°C;
- Temperature coefficient of V_{OC} (%) : −0.38/°C;
- Temperature coefficient of PM (%) : −0.47/°C;
- Temperature coefficient of JM (%) : −0.1/°C;
- Temperature coefficient of VM (%) : −0.38/°C;
- Temperature range : from -40°C to +85°C

3.2 Analytical Characteristics

The structure of PV photovoltaic module is modelled by the equivalent electrical circuit (Fig. 7) with a single diode model [3].

According to the nodes and meshes laws, we have:

$$J + J_{ph} = J_d + J_{Sh} \text{ and } V = JR_S + J_{Sh} \times R_{Sh} \quad (27)$$

Using the expression for the current-voltage characteristic of PV, we find the expression for J as:

$$J = J_{ph} - J_S \left[exp\left(\frac{q(V + R_S J)}{n K_B T}\right) - 1\right] - \frac{(V + R_S J)}{R_{Sh}} \quad (28)$$

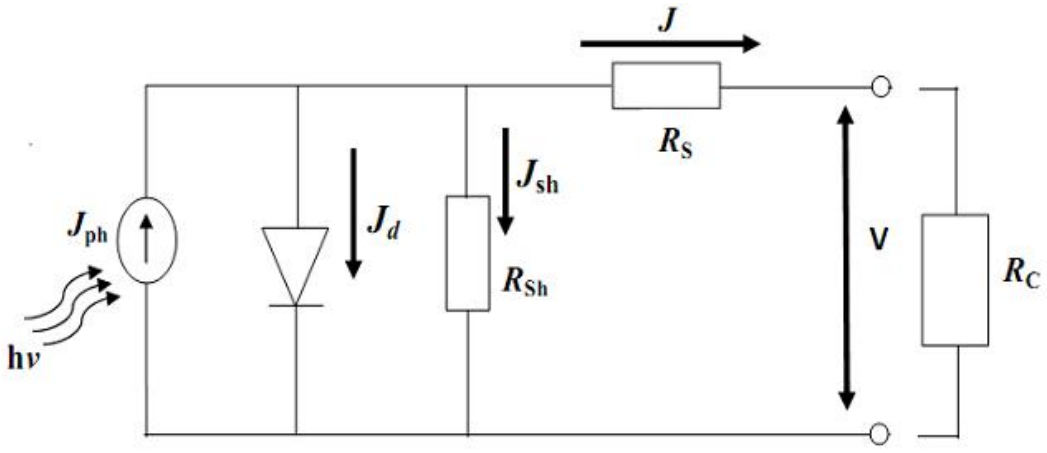

Fig. 7. Equivalent electrical circuit of PV photovoltaic module under an incident illumination

Therefore, the transcendental analytic equation for the optimal current-density J_{opt} of the ideal PV module is described by De et al. [35]:

$$J_{opt} = \frac{J_{Ph} + J_S}{1 + \frac{1}{\ln\left(\frac{J_{Ph} - J}{J_S}\right) + 1}} \quad (29)$$

with, $$V_{opt} = \frac{k\,T}{q}\ln\left(\frac{J_{Ph} - J}{J_S} + 1\right)$$

Where $J_{Ph}\,(A/cm^2)$: the photoinduced current-density determined by the spectral composition, intensity, and concentration of incident solar radiation and also by the efficiency of assembling photogenerated p-n junction charge carriers, $J_S\,(A/cm^2)$: The reverse dark photo-induced saturation current-density determined by potential and electro-physical parameters of p-n junction, **T**(°K): the PV module temperature, **k**: the Boltzmann constant; and **q** (C) is the electron charge.

When the PV module is illuminated by solar light $J_{Ph} \gg J_S$, $J_{Ph} - J \gg J_S$, the logarithm in the denominator of J_{opt} is a higher value and does not vary much with variations in J . Then, the transcendental equation is solved by stepwise approximations. For $J = 0$, we have:

$$J_{opt} = \frac{J_{Ph}}{1 + \frac{1}{\ln\left(\frac{J_{Ph}}{J_S}\right)}} \quad (30)$$

and the optimal voltage becomes:

$$V_{opt} = \frac{k\,T}{q}\left[\ln\left(\frac{J_{Ph}}{J_S}\right) - \ln\ln\left(\frac{J_{Ph}}{J_S}\right)\right] \quad (31)$$

The analytical peak power is finally expressed as:

$$P_{opt} = J_{opt} \times V_{opt} = \frac{J_{Ph}}{1 + \frac{1}{\ln\left(\frac{J_{Ph}}{J_S}\right)}} \times \frac{k\,T}{q}\left[\ln\left(\frac{J_{Ph}}{J_S}\right) - \ln\ln\left(\frac{J_{Ph}}{J_S}\right)\right] \quad (32)$$

3.3 Site Description

Benin is located between latitudes 6° and 12°30 N and longitudes 1° and 4°E, presents at south a subequatorial climate with two rainy seasons and two dry seasons. At north the climate is Sudanese with a moist season and a dry season. At south the average annual pluviometric decreases from Porto-Novo (1200 mm) to Grand-Popo (820 mm). The average monthly temperature varies from 20°C to 34°C. At north the temperatures are high, and the rainfalls are weaker between 890 and 700 mm except on the which receives on average 1300 mm in Natitingou [36].

We have simply considered dust layer thickness in our model. Since the dust effect is considered geographically site dependent, it is directly related to the local air pollution of the place where the PV system is installed.

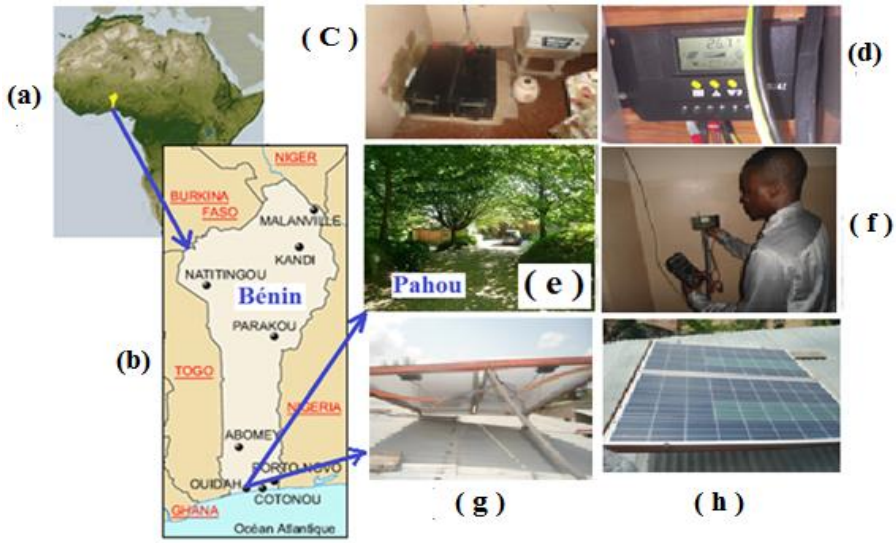

Fig. 8. (a) - Africa map showing Benin, (b) - Benin map showing Pahou locality, (C) - Storage system and Converter, (d) - Charge Controller, (e) - Pahou landscape, (f) - Phase of the electrical parameters measurement, (g) - Under module, (h) – Visual Inspection

Pahou is a hot, dusty and humid climate region where, the tiny particles of sand, trees debris, and bird's droppings are accumulating on the surface of PV modules installed, which causes a significant power loss.

We determined an expression relating the dust deposition (ω in g/m^2) to the glass transmittance reduction ($\frac{1-\tau}{\tau_{clean}}$), for three months inspired of the research works of [6]. This expression is given as follows:

$$\frac{1-\tau}{\tau_{clean}}\ (\%) = 34.37\mathrm{erf}\,(0.17\omega^{0.8473}) \qquad (33)$$

erf(x): the Gauss error function.

Next, we estimated the dust deposition density « ΔM » expressed in g/m^2 as function of the PV panel area « S », as:

$$\Delta M = \frac{\Delta m}{S} \qquad (34)$$

Δm: the total mass of dust layer on the surface of polluted PV panel.

Finally, the solar irradiance has been measured automatically by an external pyranometer or (with solar power meter) that has been placed on the solar cells glass. The modules have been cleaned at the beginning of the experiment. We effected directly the output current measure with current clamp and voltage with a multimeter regularly each week. These values are each time comparing with the initial value.

3.4 Results Simulation

It has been shown that the output power of PV cells/modules varies linearly with the solar irradiance [42]. In this study, this output power increase with increasing in the photocurrent density. Yet, in the standard conditions when the solar irradiance increases, the temperature increases, consequently the photocurrent density increases exponentially. Which confirms the result that we obtained on the (Fig. 9), using Eq. (32).

Over the period of study, the output power of modules decreased continuously due to dust accumulation (Fig. 10). Practically, from the first months of this experiment, the decrease in the output power is not very significant. This rate is constantly equal to 0.5%.

From the second month, when the dust layer, trees debris and bird's droppings on the surface of PV module are become thicker; the loss of module output power and efficiency became higher. This factor induced a decrease in intensity (Fig. 11) and a decrease in the energy production at the battery level. Our witness lamps are dimly lit showing the drop in the PV modules performance. For the other days, the observed effect is also perceptible. A significantly lower electrical energy production has been observed for PV module and the effect is primary caused by the system optimization and secondarily by the dust deposited on the PV surface. The normalized average daily energy production decreased owing to the dust deposition. This dust rate is responsible for the decrease in energy production of about 4.18%.

In addition, most of the detailed studies available in the literature were performed by means of artificial dust particles [14,23,24,43] and a few studies used natural dust [44,45] deposited on the surface of the PV module. On the other hand, in many other studies, the focus is on the physical and chemical analysis of dust particles [8,15,46], the effect of particle deposition on solar beam attenuation [47,48] or on the dust accumulation rate [18,19,45,49-53] but unfortunately, most of the data fail to take the output power losses into account, which confirms the originality of this work.

The effect of particles deposition on solar beam attenuation drops the photocurrent density and therefore, reduced the permanent internal electromagnetic field, and an attenuation of the wave propagation in the cell (Fig. 12) and (Fig. 13). This effect significantly influenced the charges carrier mobility and prevents their collection at the electrodes.

We revealed that the deposited particle size plays an important role in absorption, scattering and reflectance of the incident solar radiation. With a 73 g/m^2 deposition of cement dust resulting in an 80% drop in PV short-circuit voltage (V_{OC}); atmospheric dust with mean diameter 80 mm at 250 g/m^2 has been found to reduce the short-circuit current density (J_{SC}) by 82%. Electrical power output in the case of cement particles and carbon particles with the dust deposition density of 25 g/m^2 decreases by about 40 and 90%, respectively. Fine carbon particulates (5 mm) were found to have the most deteriorating effect on the PV efficiency (η) [14, 15,50], and a 11% reduction in transmittance has been estimated for a 5 g/m^2 dust deposition over a month under natural conditions [6].

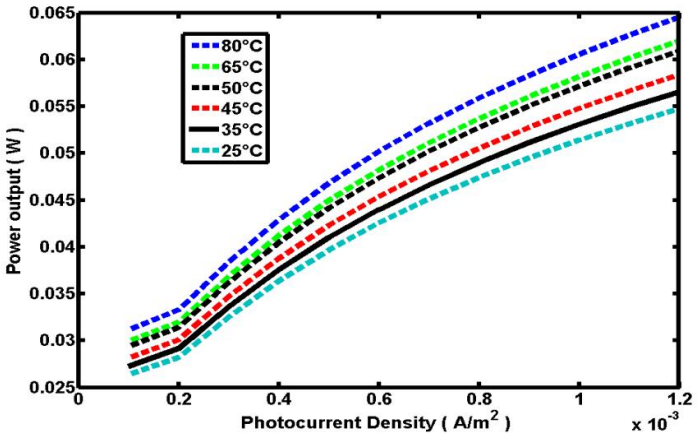

Fig. 9. Variation of power output as a function of the photocurrent density for different values of temperature

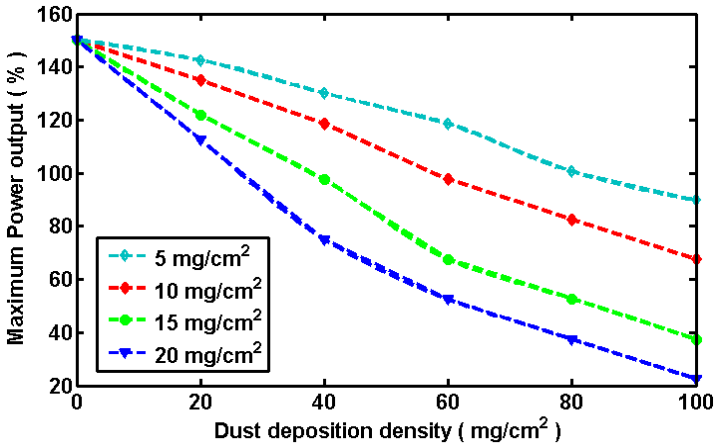

Fig. 10. Variation of output power as a function of the photocurrent density for different values of dust accumulation

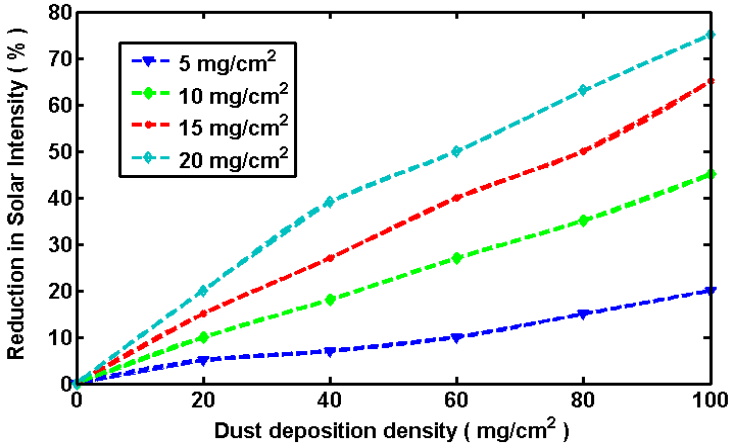

Fig. 11. Reduction in solar intensity received by the PV cell for different values of dust concentration

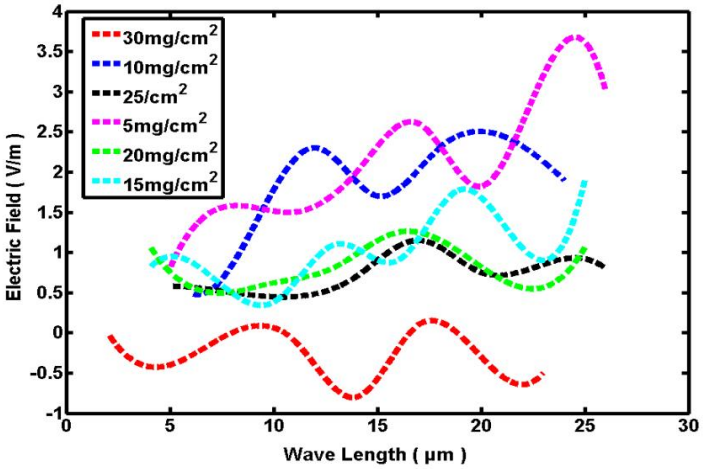

Fig. 12. Overall reduction of the wave propagation in the cell as a function of the dust layer. This figure is the numerical simulation of (Eq.19)

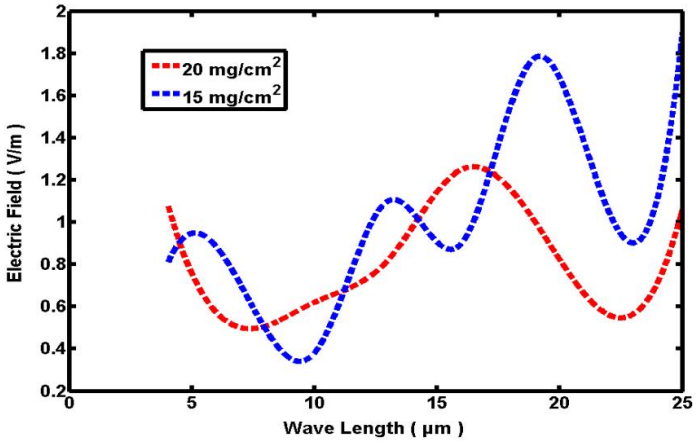

Fig. 13. Reduction of the wave propagation in the cell as a function of the dust layer: reference curves

We noted that in both cases (Fig. 12) and (Fig. 13), the wave amplitude decreases when the dust thickness increases. This effect is responsible for the decrease in energy production of about 4.18% per week.

Due to the stochastic nature of variations of the environmental condition including pollution, the dust deposition imparts this nature. The total weekly dust mass deposited at the PV module surface depends on the air pollution, wind speed, humidity and what are the most important rainfalls which occurred during the period of analysis almost every week. Finally, we can assert that the performance of PV cells/ modules depends on the environmental conditions and seasons of year [1,54,55,56].

4. CONCLUSIONS

We investigated analytically the performance degradation of the BPS150-36 Polycrystalline silicon module, caused by the natural dust deposition effects on the transparent panel surface. Matrix-Transfer theory with the cubic spline interpolation method has been exploited for data correlation. Matlab software has been used for numerical simulation results.

The results obtained show:

- A significant decrease in the power output;
- A decrease in intensity and a decrease in the energy production at the batteries level;

- The normalized average daily energy production decreased owing to the dust deposition. This dust rate is responsible for the decrease in energy production of about 4.18%.
- A drop of the permanent internal electromagnetic field, and an attenuation of the wave propagation in the cell. This strongly depends on the dust layer on the panel's surface. These effects significantly influence the charges carrier mobility and prevent their collection at the electrodes.

PV module performance decrease influenced by dust constitutes a local phenomenon and differ significantly from region to region

The exposure time does not provide sufficient information about solar radiation attenuation due to dust deposition. It is very difficult to create a general model for dust deposition and dust-related PV system efficiency reduction.

Future work can be about:

1- Extensions to the model,
2- Improvement of the analytical results,
3- Analytical Modeling of Damp-Heat Effects into Polycrystalline Silicon PV Cells/Modules will be studied.

ACKNOWLEDGEMENTS

I grateful to Professor Basile Bruno Kounouhéwa and Dr. Vianou Irénée Madogni for their efforts in the realization of this work. I acknowledge “Laboratoire de Physique du Rayonnement LPR, FAST-UAC 01BP 526 Cotonou, Benin”.

COMPETING INTERESTS

Authors have declared that no competing interests exist.

REFERENCES

1. Cabanillas RE, Munguı’a H. Dust accumulation effect on efficiency of Si photovoltaic modules. Journal of Renewable Energy and Sustainable Energy. 2011;3:043114.
2. Sadok M, Mehdaoui A. Outdoor testing of photovoltaic arrays in the Saharan region. Renewable Energy. 2008;33:2516-2524.
3. Madogni VI, Kounouhéwa B, Yakoub IA, Agbomahéna M, Houngninou E, Kouchadé C, Awanou CN. Modèle analytique pour l’étude de la dégradation de la performance des cellules photovoltaïques au silicium monocristallin. Afrique Science. 2016;12:182-200.
4. Mohamed AO, Hasan A, Effect of dust accumulation on performance of photo-voltaic solar modules in Sahara environ-ment. Journal of Basic and Applied Scientific Research. 2012;2:11030-11036.
5. Mekhilef S, Saidurb R, Kamalisarvestani M. Effect of dust, humidity and air velocity on efficiency of photovoltaic cells. Renewable and Sustainable Energy Reviews. 2012;16:2920-2925.
6. Mani M, Pillai R. Impact of dust on solar photovoltaic (PV) performance: Research status, challenges and recommendations. Renewable and Sustainable Energy Reviews. 2010;14:3124-31.
7. Kazem HA, Khatib T, Sopian K, Buttinger F, Elmenreich W, Albusaidi AS. Effect of dust deposition on the performance of multi-crystalline photovoltaic modules based on experimental measurements. International Journal of Renewable Energy Research. 2013;3:850-853.
8. Kaldellis JK, Kapsali M. Simulating the dust effect on the energy performance of photovoltaic generators based on experimental measurements. Energy. 2011;36:5154-5l61.
9. Travis S, Al-Qaraghuli A, Lawrence LK. A comprehensive review of the impact of dust on the use of solar energy: History, investigations, results, literature, and mitigation approaches. Renewable and Sustainable Energy Reviews. 2013;22: 698-733.
10. Garg HP. Effect of dirt on transparent covers in flat plate solar energy collectors. Solar Energy. 1974;15:299-302.
11. Said S, Effect of dust accumulation on performances of thermal and PV flat plate collectors. Applied Energy. 1990;37:73-84.
12. Nahar N, Gupta J. Effect of dust on transmittance of glazing materials for solar collectors under arid zone conditions of India. Solar Wind Technology. 1990;7: 237-43.
13. Michalsky JJ, Perez R, Stewart R, LeBaron BA, Harrison L. Design and development of a rotating shadow band radiometer solar radiation/daylight network. Solar Energy. 1988;41:577-81.
14. El-Shobokshy MS, Hussein FM. Effect of the dust with different physical properties

on the performance of photovoltaic cells. Solar Energy. 1993;51:505-11.
15. El-Shobokshy MS, Hussein FM. Degradation of photovoltaic cell performance due to dust deposition on to its surface. Renewable Energy. 1993;3:585-90.
16. Goossens D, Offer ZY, Zangvil A. Wind tunnel experiments and field investigations of eolian dust deposition on photovoltaic solar collectors. Solar Energy. 1993;50: 75-84.
17. Al-Hasan AY. A new correlation for direct beam solar radiation received by Photovoltaic panel with sand dust accumulated on its surface. Solar Energy. 1998;63:323-33.
18. Mastekbayeva GA, Kumar S. Effect of dust on the transmittance of low density polyethylene glazing in a tropical climate. Solar Energy. 2000;68:135-41.
19. Hegazy AA. Effect of dust accumulation on solar transmittance through glass covers of plate-type collectors. Renewable Energy. 2001;22:525-40.
20. Hassan AH, Rahoma UA, Elminir HK, Fathy AM. Effect of airborne dust concentration on the performance of PV modules. Journal of the Astronomical Society of Egypt. 2005;13:24-38.
21. Elminir HK, Ghitas AE, Hamid RH, El-Hussainy F, Beheary MM, Abdel Moneim KM. Effect of dust on the transparent cover of solar collectors. Energy Conversion Management. 2006;47:3192-203.
22. Kymakis E, Kalykakis S, Papazoglou TM. Performance analysis of a grid connected Photovoltaic Park on the island of crete. Energy Conversion and Management. 2009;50:433-8.
23. Kaldellis JK, Fragos P. Ash deposition impact on the energy performance of photovoltaic generators. Journal Cleaner Production. 2011;19:311-317.
24. Kaldellis JK, Fragos P, Kapsali M. Systematic experimental study of the pollution deposition impact on the energy yield of photovoltaic installations. Renewable Energy. 2011;36:2717-2724.
25. Beattie NS, Moir RS, Chacko C, Buffoni G, Roberts SH, Pearsalla NM. Understanding the effects of sand and dust accumulation on photovoltaic modules. Renewable Energy. 2012;48:448-452.
26. Chitlange M, Pajgade P. Strength appraisal of artificial sand as fine aggregate in SFRC. ARPN Journal of Engineering and Applied Sciences. 2010; 5:34-38.
27. Belyakova L, Varvarin A. Surfaces properties of silica gels modified with hydrophobic groups. Colloids and Surfaces A: Physicochemical and Engineering Aspects. 1999;154:285-294.
28. Kralj D, Vdović N. The influence of some naturally occurring minerals on the precipitation of calcium carbonate polymorphs. Water Research. 2000;34:179-184.
29. Shockley W, Queisser HJ. Detailed balance limit of efficiency of p-n junction solar cells. Journal of Applied Physics. 1961;32:510-519.
30. Deibel C, Dyakonov V. Polymer-fullerene bulk heterojunction solar cells. Reports on Progress in Physics. 2010;73:096401.
31. Nyman M. Interfacial effects in organic solar cells. PhD dissertation, Abo Akademi University, Finland; 2015.
32. Heavens OS. Optical properties of thin solid films. Dover, New York; 1965.
33. Pettersson LAA, Roman LS, Inganas O. Modeling photocurrent action spectra of photovoltaic devices based on organic thin films. Journal of Applied Physics. 1999;86: 487-496.
34. Casanova JZ, Piliougine M, Carretero J, Bernaola P, Carpena P, Löpez LM, Cardona MS. Analysis of dust losses in photovoltaic modules. Word Renewable Energy Congress. Sweden 2990; 2011.
35. De Soto W, Klein SA, Beckman WA. Improvement and validation of a model for photovoltaic array performance. Solar Energy. 2006;80:78-88.
36. Duffie JA, Beckman WA. Solar engineering of thermal processes. second ed. John Wiley & Sons Inc., New York; 1991.
37. Rachid K, Hamid EH. Solar cells performance reduction under the effect of dust in Jazan region. Journal of Fundamentals of Renewable Energy and Applications. 2017;7:1-4.
38. Sloane CS, Watson JG, Chow J, Pritchett LC, Richards LW. Sized- segregated fine particle measurements by chemical species and their impact on visibility impairment in denver. Atmospheric Environment. 1991;25A:1013-1024.
39. Bohren CF, Huffman DR. Absorption and scattering of light by small particles. John Wiley & Sons, New York; 1983.

40. Van de Hulst HC. Light scattering by small particles. Quarterly Journal of the Royal Meteorological Society. 1958;84:198-199.
41. Saito J, Sasaki H, Yachi T. Degradation of photovoltaic module output power by micro particles. 37th IEEE Photovoltaic Specialists Conference; 2011.
42. Bashir MA, Ali HM, Muzaffar A, Siddiqui AM. An experimental investigation of performance of photovoltaic modules in Pakistan. Thermal Science. 2015;19: S525-S534.
43. Sayyah A, Horenstein MN, Mazumder MK. Energy yield loss caused by dust deposition on photovoltaic panels. Solar Energy. 2014;107:576-604.
44. Ali HM, Zafar MA, Bashir MA, Nasir MA, Ali M, Siddiqui AM. Effect of dust deposition on the performance of photovoltaic modules in Taxila, Pakistan. Thermal Science. 2015a;46-46.
45. Kaldellis JK, Kokala A, Kapsali M. Natural air pollution deposition impact on the efficiency of PV panels in urban environment. Fresenius Environ Bull. 2010;19: 2864-2872.
46. Tian W, Wang Y, Ren J, Zhu L. Effect of urban climate on building integrated photovoltaics performance. Energy Conversion and Management. 2007;48:1-8.
47. Kumar ES, Sarkar B, Behera D. Soiling and dust impact on the efficiency and the maximum power point in the photovoltaic modules. International Journal of Engineering. 2013;2:1-8.
48. Ketjoy N, Konyu M. Study of dust effect on photovoltaic module for photovoltaic power plant. Energy Procedia. 2014;52:431-437.
49. Javed W, Wubulikasimu Y, Figgis B, Guo B. Characterization of dust accumulated on photovoltaic panels in Doha, Qatar. Solar Energy. 2017;142:123-135.
50. Saidan M, Albaali AG, Alasis E, Kaldellis J K. Experimental study on the effect of dust deposition on solar photovoltaic panels in desert environment. Renewable Energy. 2016;92:499-505.
51. Boppana S. Outdoor soiling loss characterization and statistical risk analysis of photovoltaic power plants. Arizona State University, Tempe; 2015.
52. Weber B, Quiñones A, Almanza R, Duran MD. Performance reduction of PV systems by dust deposition. Energy Procedia. 2014; 57:99-108.
53. Boyle L, Flinchpaugh H, Hannigan MP. Natural soiling of photovoltaic cover plates and the impact on transmission. Renewable Energy. 2015;77:166-173.
54. Ali HM, Mubashar M, Muhammad AB, Muzaffar A, Aysha MS. Outdoor testing of photovoltaic modules during summer in Taxila, Pakistan. Thermal Science. 2016; 20:165-173.
55. Muhammad BC, Ali HM, Muzaffar A, Muhammad AB. Experimental investigation of monocrystalline and polycrystalline solar modules at different inclination angles. Journal of Thermal Engineering. 2018;4; 2137-2148.
56. Muhammad AB, Ali HM, Shahid K, Muzaffar A, Aysha MS. Comparison of performance measurements of photovoltaic modules during winter months in Taxila, Pakistan. International Journal of Photoenergy. 2014;1-8.

© 2018 Capo-Chichi et al.; This is an Open Access article distributed under the terms of the Creative Commons Attribution License (http://creativecommons.org/licenses/by/4.0), which permits unrestricted use, distribution, and reproduction in any medium, provided the original work is properly cited.

Peer-review history:
The peer review history for this paper can be accessed here:
http://www.sciencedomain.org/review-history/27956